ALICE-PUBLIC-2013-002
LHCb-CONF-2013-013
December 21, 2013

Reference pp cross-sections for J/ψ studies in proton-lead collisions at $\sqrt{s_{NN}} = 5.02\,\text{TeV}$ and comparisons between ALICE and LHCb results

The ALICE collaboration †
The LHCb collaboration ‡

Abstract

The ALICE and LHCb collaborations have studied J/ψ production at forward rapidities in proton-lead collisions at $\sqrt{s} = 5.02\,\text{TeV}$ using the dimuon channel. The evaluation of cold nuclear matter effects requires the knowledge of the corresponding J/ψ cross-section in pp collisions at the same centre-of-mass energy and in the same kinematic range. In this note the interpolation procedure used to determine this quantity and the related consistency checks are described. Finally, the results from the two experiments on nuclear modification factors are shortly summarized and found to be in good agreement.

† Contact authors: Roberta Arnaldi, arnaldi@to.infn.it and Enrico Scomparin, scompar@to.infn.it.
‡ Contact authors: Fanfan Jing, fanfan.jing@cern.ch, Michael Schmelling, Michael.Schmelling@mpi-hd.mpg.de.

1 Introduction

The analysis of high energy proton-lead (pPb) collisions allows to study the influence of cold nuclear matter effects on hard processes and is thus important for the interpretation of the related quark-gluon plasma signatures in heavy-ion collisions [1].

The J/ψ meson is an ideal tracer for these kinds of studies [2] since it is a tightly bound system of heavy quarks which are not present in the initial state. The production of the primary heavy quark pair is sensitive to the parton densities in the collision partners, which can be altered by nuclear shadowing effects [3], while the subsequent formation and propagation of the J/ψ meson is affected by the nuclear environment which may lead to its dissociation [4]. In addition, parton energy loss in the initial and/or final state can also play a role in determining the kinematic distribution of the measured J/ψ [5]. Further information can be gained by comparing prompt J/ψ production and J/ψ mesons from b-hadron decays. The latter source is sensitive to nuclear processes affecting the production of the parent b-quark, including shadowing, and to its energy loss in cold nuclear matter [6].

The observable commonly used to quantify the effects described above is the nuclear modification factor. When expressed as a function of the rapidity y it is defined as

$$R_{p\mathrm{Pb}}(y) = \frac{1}{A}\frac{\mathrm{d}\sigma^{\mathrm{J}/\psi}_{p\mathrm{Pb}}/\mathrm{d}y}{\mathrm{d}\sigma^{\mathrm{J}/\psi}_{pp}/\mathrm{d}y}, \tag{1}$$

where A is the atomic number of the colliding nucleus. Another good observable is the forward to backward production ratio

$$R_{\mathrm{FB}}(|y|) = \frac{\mathrm{d}\sigma_{p\mathrm{Pb}}(+|y|)/\mathrm{d}y}{\mathrm{d}\sigma_{p\mathrm{Pb}}(-|y|)/\mathrm{d}y}\,, \tag{2}$$

which is also sensitive to the relative strength of cold nuclear matter effects but does not depend on the pp cross-section and its related uncertainties. Note that rapidity always refers to the nucleon-nucleon centre-of-mass system with the direction of the proton momentum defining positive rapidity. The ALICE and LHCb collaborations have studied J/ψ production in pPb collisions at $\sqrt{s} = 5.02\,\mathrm{TeV}$ [7,8]. The determination of the nuclear modification factor requires knowledge of the pp cross-sections at the same centre-of-mass energy, where until now no experimental data exist. As a consequence the available cross-section measurements at $\sqrt{s} = 2.76, 7\,\mathrm{and}\,8\,\mathrm{TeV}$ [9–13] have to be interpolated. This document focuses on the interpolation strategies employed by the ALICE and LHCb collaborations and compares the results obtained by the two experiments for the nuclear modification factors and the forward-backward production ratios. The physics is discussed in greater depth in the individual ALICE/LHCb publications.

In this note we are consistently referring to a nucleon-nucleon centre-of-mass energy of $\sqrt{s} = 5.02\,\mathrm{TeV}$, which is the nominal value when colliding 4 TeV protons on ^{208}Pb nuclei, i.e. the two decimal digits do not reflect the actual precision to which the centre-of-mass energy is known. In fact, taking the measured energy of the proton beam as reported in

Table 1: Existing J/ψ cross-section measurements in $2.5 < y < 4.0$ from ALICE [9, 10] and LHCb [11–13]. The LHCb cross-section at $\sqrt{s} = 2.76\,\text{TeV}$ was obtained by rescaling the measured value to the rapidity interval $2.5 < y < 4.0$. At the other centre-of-mass energies the cross-sections were calculated by integrating the published double differential measurements over the same rapidity range. The first quoted uncertainty is statistical and the second is systematic.

Experiment	$\sqrt{s}$ [TeV]	process	$\sigma(J/\psi)$ [μb]
ALICE	2.76	inclusive	$3.34 \pm 0.13 \pm 0.27$
ALICE	7	inclusive	$6.78 \pm 0.04 \pm 0.64$
LHCb	2.76	inclusive	$3.48 \pm 0.06 \pm 0.27$
LHCb	7	inclusive	$6.55 \pm 0.01 \pm 0.37$
LHCb	8	inclusive	$7.59 \pm 0.01 \pm 0.55$
LHCb	2.76	prompt	$3.23 \pm 0.06 \pm 0.26$
LHCb	7	prompt	$5.89 \pm 0.01 \pm 0.33$
LHCb	8	prompt	$6.79 \pm 0.01 \pm 0.49$
LHCb	2.76	J/ψ from b	$0.248 \pm 0.022 \pm 0.034$
LHCb	7	J/ψ from b	$0.660 \pm 0.005 \pm 0.050$
LHCb	8	J/ψ from b	$0.796 \pm 0.002 \pm 0.058$

Ref. [14], $E_p = 3988 \pm 26\,\text{GeV}$ and the corresponding nucleon energy of the Pb beam of $E_{\text{Pb}} = 1572 \pm 10\,\text{GeV}$, one obtains $\sqrt{s} = 5.01 \pm 0.03\,\text{TeV}$. For their publication ALICE [7] has chosen to quote the nominal centre-of-mass energy, while LHCb [8] has decided to quote $\sqrt{s} = 5\,\text{TeV}$, which is consistent with the actual value of the nucleon-nucleon centre-of-mass energy and does not suggest a precision of more than one decimal digit. For the physics which is being discussed here, the difference is irrelevant.

2 Interpolation with $\sqrt{s}$ of integrated cross-sections

For the cross-section interpolation three types of functions are considered

$$\sigma(\sqrt{s}) = \begin{cases} p_0 + \sqrt{s}\,p_1 & \text{linear} \\ (\sqrt{s}/p_0)^{p_1} & \text{power law} \\ p_0(1 - \exp(-\sqrt{s}/p_1)) & \text{exponential .} \end{cases} \tag{3}$$

All three functions have two free parameters. The linear function as a 1^{st}-order Taylor expansion is safe for interpolation over small regions. The power law automatically implements the constraint that the cross-section is zero at zero energy, and it is invariant when interpolating in s rather than $\sqrt{s}$. Also, there are other quantities like total cross-sections [15] or total multiplicities [16] where power-law functions provide good descriptions of experimental data. The exponential interpolation also satisfies $\sigma(s = 0) = 0$ and at the same time forces a negative curvature. In contrast, the linear function has no curvature while the power law can have both positive and negative curvature. The three functions thus form a convenient set to probe the systematic uncertainty related to the interpolation.

Table 2: Cross-sections in units of μb for prompt J/ψ production at $\sqrt{s} = 2.76$, 5.02 and 7 TeV as predicted by the LO-CEM and FONLL models. The LO-CEM/CTEQ6L predictions for factorization scales $\mu_{\rm F} = m_c/2$ and $\mu_{\rm F} = m_c$ are identical and listed only once. The minimum and maximum values for FONLL result from varying the renormalization scale $\mu_{\rm R}$ and the factorization scale $\mu_{\rm F}$ in the range $\mu_0/2 < \mu_{\rm R}, \mu_{\rm F} < 2\mu_0$ with the constraint $1/2 < \mu_R/\mu_F < 2$, having defined μ_0 by $\mu_0^2 = {p_{\rm T}}^2 + m_c^2$.

Model/PDF	factorization scale	$\sigma(2.76\,\text{TeV})$	$\sigma(5.02\,\text{TeV})$	$\sigma(7\,\text{TeV})$
LO-CEM/CTEQ6L	$m_c, m_c/2$	4.271	5.300	5.815
LO-CEM/CTEQ6L	$2m_c$	3.382	5.300	6.619
LO-CEM/MRST98L	$m_c/2$	4.294	5.300	5.837
LO-CEM/MRST98L	m_c	3.880	5.300	6.188
LO-CEM/MRST98L	$2m_c$	3.236	5.300	6.820
LO-CEM/CTEQ5L	$m_c/2$	3.891	5.300	6.180
LO-CEM/CTEQ5L	m_c	3.604	5.300	6.450
LO-CEM/CTEQ5L	$2m_c$	3.138	5.300	6.928
LO-CEM/MRST01L	$m_c/2$	4.584	5.300	5.586
LO-CEM/MRST01L	m_c	4.018	5.300	6.131
LO-CEM/MRST01L	$2m_c$	3.391	5.300	6.670
LO-CEM/GRV98L	$m_c/2$	3.697	5.300	6.412
LO-CEM/GRV98L	m_c	3.352	5.300	6.765
LO-CEM/GRV98L	$2m_c$	3.029	5.300	7.124
FONLL	(nominal)	3.331	5.300	6.670
FONLL	(min)	3.872	5.300	6.142
FONLL	(max)	3.413	5.300	6.587

In the remainder of this section we will test the use of the chosen interpolating functions against theoretical calculations (Section 2.1). Then we determine the J/ψ cross-section in pp collisions at $\sqrt{s} = 5.02$ TeV in the rapidity range $2.5 < y < 4.0$, interpolating the experimental results, summarized in Tab. 1, from both ALICE (Section 2.2) and LHCb (Section 2.3). For LHCb, this y-range corresponds, in absolute value, to the ones studied in pPb collisions ($2.5 < y < 4.0, -4.0 < y < -2.5$). For ALICE, the rapidity ranges probed in pPb collisions are slightly different ($2.03 < y < 3.53, -4.46 < y < -2.96$), requiring a further extrapolation step, described in Section 3.

2.1 Theoretical models versus phenomenological functions

As a first step we check how well the interpolation functions introduced above are able to reproduce the energy dependence of theoretical calculations of prompt J/ψ production. Theoretical predictions for the rapidity range $2.5 < y < 4.0$, integrated over transverse momentum, have been obtained for the Leading Order Colour Evaporation Model (LO-CEM) [17]. In addition, the FONLL [18] model has been used. As this model gives predictions for the open charm cross-sections, it is assumed that the fraction of $c\bar{c}$-pairs

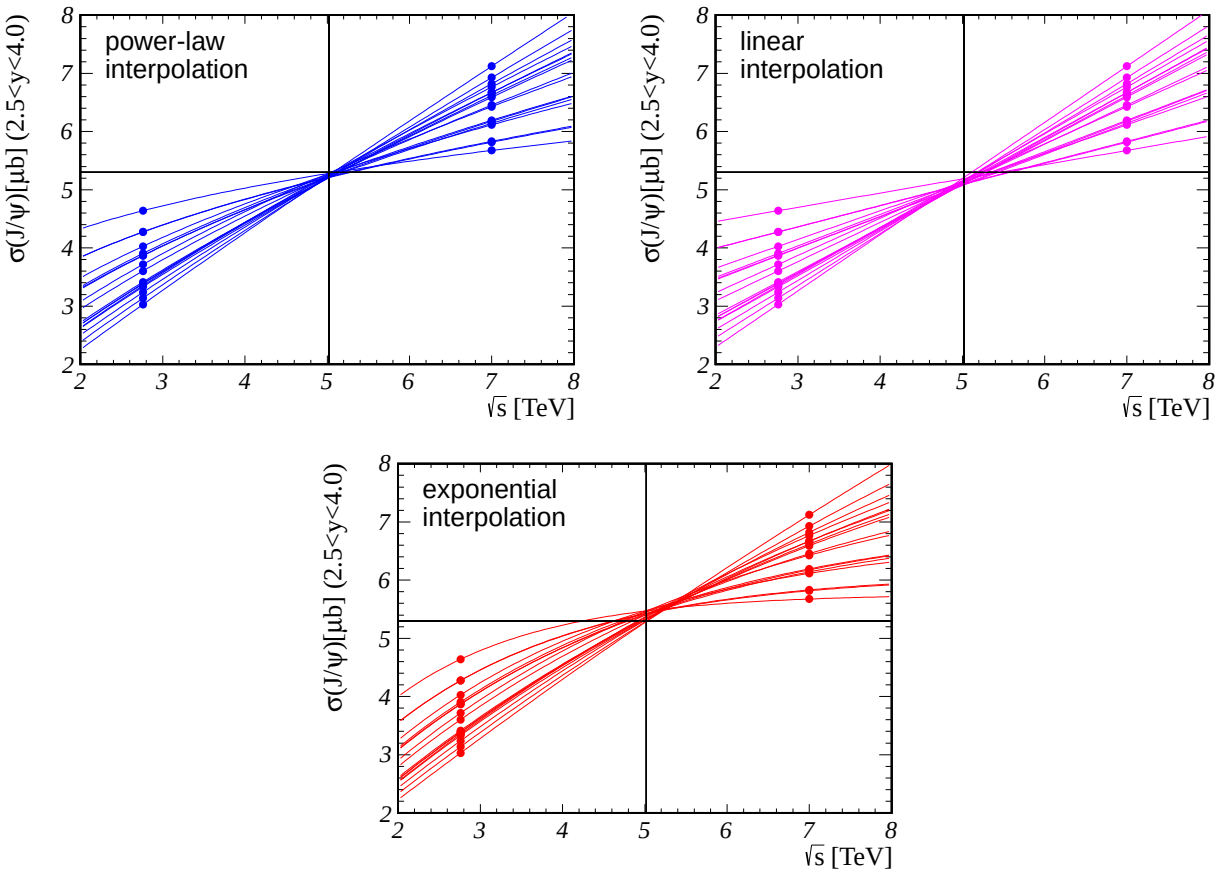

Figure 1: Comparison of power-law (top left), linear (top right) and exponential (bottom) interpolations for the energy dependence of the J/ψ production cross-sections for the theoretical predictions given in Tab. 2. Ideally all curves should go through $\sigma(\sqrt{s} = 5.02\,\text{TeV}) = 5.3\,\mu\text{b}$.

which end up in charmonium states is constant versus $\sqrt{s}$ [19]. The predictions are very sensitive to the choice of the renormalization and the factorization scale, which results in cross-section predictions varying over two orders of magnitude. The predictions for the energy dependence, however, are much more stable. Since the absolute cross-sections are almost unconstrained, for this study all predictions have been scaled such that the cross-section at $\sqrt{s} = 5.02\,\text{TeV}$ takes on an arbitrary value close to the actual interpolation result, $\sigma(\sqrt{s} = 5.02\,\text{TeV}) = 5.3\,\mu\text{b}$. Table 2 lists the available predictions, which were determined for the energy range where both ALICE and LHCb have pp results. They do not include a contribution from b-decays, which is anyway small and was found to change by only 2% between $\sqrt{s} = 2.76$ and 7 TeV [11, 12], therefore not affecting the shape of the $\sqrt{s}$-dependence.

For the check of the interpolation the two free parameters of each interpolation function shown in Eq. 3 are determined to reproduce the two cross-section values at $\sqrt{s} = 2.76$ and 7 TeV, and the interpolated value at $\sqrt{s} = 5.02\,\text{TeV}$ compared to the fixed reference value. Figure 1 shows the quality of the interpolation for all cases. Ideally all curves

should go through the point (5.02 TeV, 5.3 μb) marked by the cross line. One clearly sees that the power-law parameterization on average gets closest to the reference point. The linear fit clearly underestimates the cross-section, while the exponential ansatz slightly overestimates it.

Quantitatively, the difference between interpolation and reference cross-section at $\sqrt{s} = 5.02\,\text{TeV}$ are $(-1.2 \pm 0.5)\,\%$ for the power-law interpolation, $(-3.1 \pm 0.7)\,\%$ for the linear and $(+1.7 \pm 1.1)\,\%$ for the exponential ansatz, where the uncertainty is the root-mean-square (RMS) scatter of the interpolated values. A convenient measure to quantify the systematic uncertainty of the interpolation is the quadratic sum of offset and RMS-scatter, which is 1.3 % for the power-law interpolation, 3.2 % for the linear interpolation and 2.0 % for the exponential interpolation. The study shows that over the energy range under discussion cross-section interpolation using a power-law ansatz is good to better than 2 %, and that taking the difference between the power law and any of the alternatives is a conservative estimate for the theoretical uncertainties of the interpolation.

2.2 ALICE cross-section interpolation

The above studies justify using the phenomenological functions defined in Eq. 3 to estimate the J/ψ production cross-section at $\sqrt{s} = 5.02\,\text{TeV}$ from existing measurements, which for ALICE currently exist only for centre-of-mass energies of $\sqrt{s} = 2.76$ and 7 TeV [9, 10]. The phenomenological functions were adjusted to the experimental data by means of least squares fits, using as uncertainties in the fit procedure the quadratic sum of statistical and uncorrelated systematic uncertainties. A 5% correlated uncertainty between the $\sqrt{s} = 2.76$ and 7 TeV data points, related to a combination of uncertainties on tracking and triggering efficiencies, and to the uncertainty on the branching ratio to muon pairs, was then added in quadrature to the result of the interpolations. The value of the interpolated cross section was finally determined as the weighted average of the results obtained using the different phenomenological functions, with the weights given by the inverse of the variances of the individual points. In addition, a 0.10 µb uncertainty is assigned from the maximum deviation between the average and either of the individual fits. With this procedure, the uncertainty on the interpolated cross section at $\sqrt{s} = 5.02\,\text{TeV}$ is 7.9%. The ALICE results are shown in Fig. 2 and listed in Tab. 3.

Table 3: Cross-section interpolation of the ALICE data. See text for details on the assignment of the uncertainties.

model	cross-section [µb]
linear	5.17 ± 0.41
power law	5.26 ± 0.40
exponential	5.38 ± 0.40
average	$5.28 \pm 0.40 \pm 0.10$

The cross-section interpolation discussed so far employs existing calculations only to motivate the functional form for the interpolation. As such it is relatively model

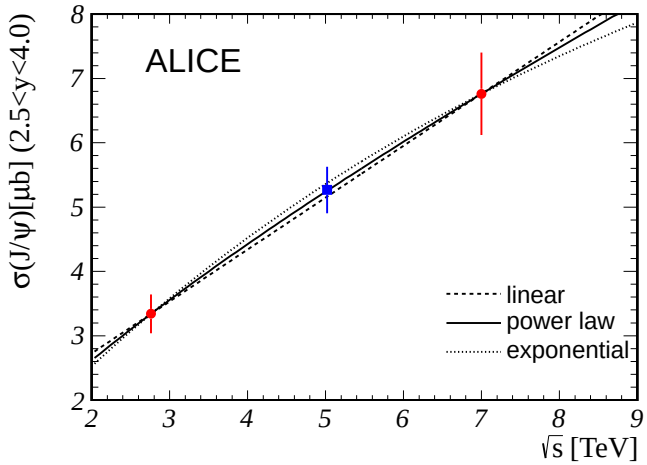

Figure 2: Cross-section interpolation for the ALICE data. The point at $\sqrt{s} = 5.02\,\text{TeV}$ is the result of the interpolation procedure, the error bar shows the result from error propagation of the experimental uncertainties of the measurements at $\sqrt{s} = 2.76$ and $7\,\text{TeV}$.

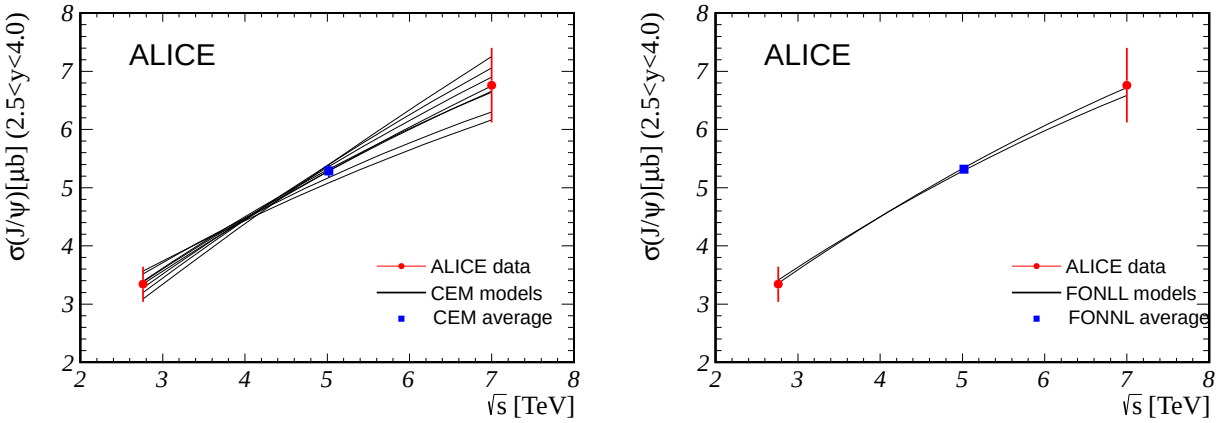

Figure 3: Cross-section interpolation by fitting theoretical predictions to the ALICE data points.

independent and allows one to derive an effective parameterization of the energy dependence of the J/ψ production cross-section which is driven by experimental data.

As a cross-check, the alternative approach that can be followed is to use the calculations directly, adjust the normalization to get an optimal description of the existing data and then take the predicted value at $\sqrt{s} = 5.02\,\text{TeV}$ as an estimate for the cross-section at the intermediate point. Although somewhat redundant when good models for the actual functional form of the energy dependence of the cross-section exist, this approach is attractive since even for only two data points, fitting the normalization leaves one degree of freedom to judge the quality of the fit. The higher statistical precision of a one parameter fit, however, is somewhat compromised by the fact that in this case also a systematic error due to the choice of the theoretical model has to be added.

In this approach, only models which provide a good description of the experimental

data (with $\chi^2/\mathrm{NDF} < 3$, where NDF is the number of degrees of freedom in the fit) are used. The fits were done separately for the CEM- and FONLL-based predictions.

Figure 3 shows how the models compare to the experimental data. The predicted cross-section is taken as the average of the models that describe the data. For the CEM-family one finds $\sigma(5.02\,\mathrm{TeV}) = 5.29 \pm 0.10\,\mu\mathrm{b}$ and for the FONLL-predictions $\sigma(5.02\,\mathrm{TeV}) = 5.32 \pm 0.02\,\mu\mathrm{b}$, where the uncertainty is the RMS-scatter of the actual values.

The interpolated values for both types of theoretical models are in good agreement with the phenomenological interpolation discussed in the previous section, which again justifies the heuristic procedure. Nevertheless, the maximum deviation between average of the phenomenological fits and either of the averages to the theoretical models, $\Delta\sigma = 0.05\,\mu\mathrm{b}$ is conservatively assigned as an additional systematic error for the interpolation. The final estimate for the inclusive J/ψ cross-section at $\sqrt{s} = 5.02\,\mathrm{TeV}$ in $2.5 < y < 4.0$ based on the ALICE measurements at 2.76 and 7 TeV in the same y-range therefore becomes

$$\sigma_{\mathrm{incl}} = 5.28 \pm 0.40_{\mathrm{exp}} \pm 0.10_{\mathrm{inter}} \pm 0.05_{\mathrm{theo}}\,\mu\mathrm{b} = 5.28 \pm 0.42\,\mu\mathrm{b}\ .$$

2.3 LHCb cross-section interpolation

The LHCb collaboration has chosen to perform the cross-section interpolation based entirely on the phenomenological functions introduced above. Here measurements exist for the three energies [11–13], and the only input taken from theory is the generic functional form of the energy dependence of the cross-section, i.e. the theory uncertainty assigned by ALICE does not enter. This approach is chosen as three data points are available to perform a two-parameter fit; in such a case an assessment of the quality of the fit is possible without referring to a specific set of theoretical predictions. The nominal result is taken to be that from the power-law interpolation, and the maximum difference to any of the other options is assigned as systematic uncertainty. The results of the different fits are listed in Tab. 4 and displayed in Fig. 4.

For the determination of the uncertainties of the interpolated cross-sections, the correlations in the systematic uncertainties of the measurements at different energies are estimated by assuming for any common source of systematics between two measurements the smaller value to be fully correlated. Such a procedure applied to the modelling of the signal shape in the analysis, muon-identification and tracking efficiency, vertexing, global event cuts, branching ratio and trigger gives a 2.2% uncertainty to be correlated between 2.76 and 7 TeV, 3.4% between 2.76 and 8 TeV and 2.4% between 7 and 8 TeV. Given that the trigger was the same at 2.76 and 8 TeV, but different for the 7 TeV data, the systematic error due to the trigger efficiency was assumed to be fully correlated between 2.76 and 8 TeV and uncorrelated to the 7 TeV measurements. As the dominant uncertainties in the integrated luminosity for the three data sample are independent, the systematic uncertainties on the luminosity are treated as uncorrelated.

The final results for the interpolated cross-sections at $\sqrt{s} = 5.02\,\mathrm{TeV}$ for the rapidity

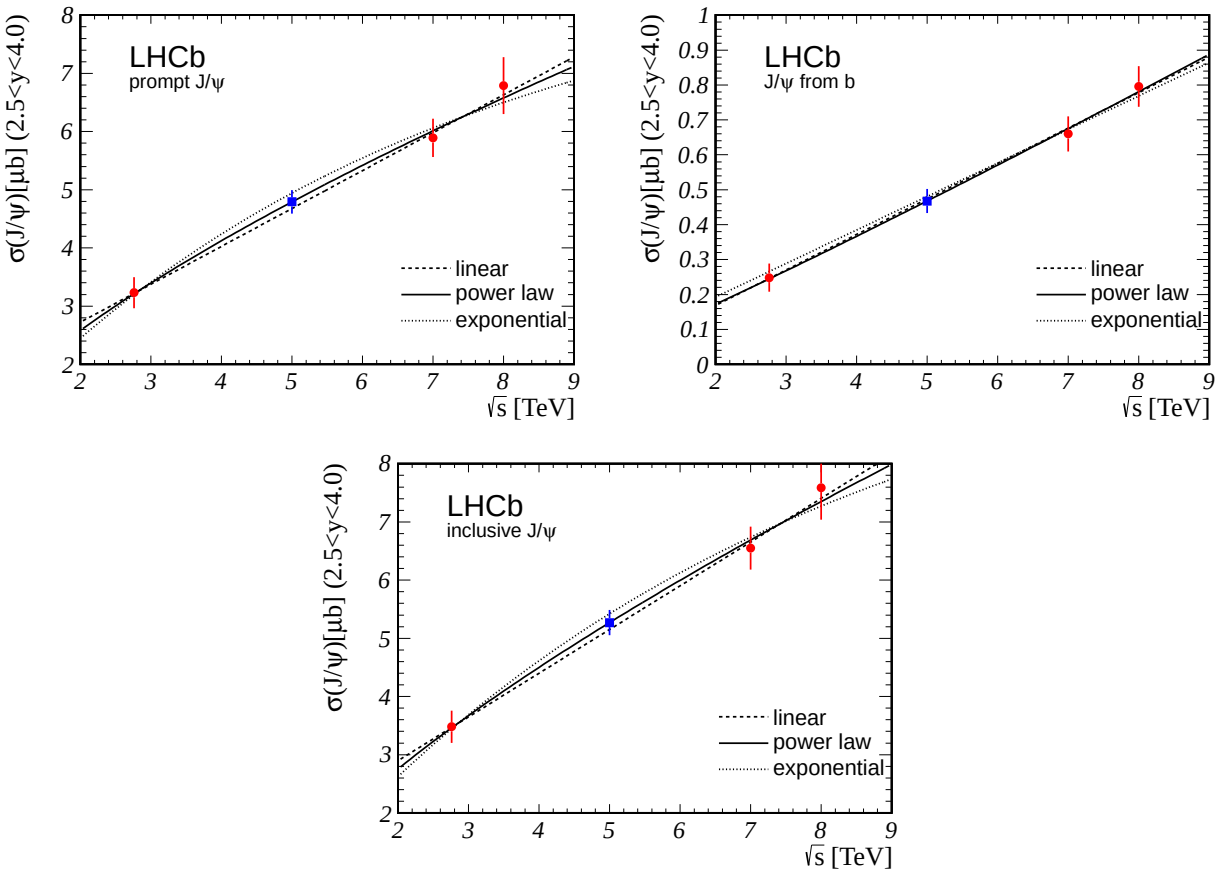

Figure 4: Cross-section interpolation for the LHCb data using three phenomenological models. The upper row shows the results for prompt J/ψ production (top left) and for J/ψ mesons from b-hadron decays (top right). The bottom row plot shows the interpolation for inclusive J/ψ production. The points at $\sqrt{s} = 5.02\,\text{TeV}$ are the nominal results of the interpolation procedure, the error bar is the result from error propagation of the experimental uncertainties of the measurements at $\sqrt{s} = 2.76$, 7 and 8 TeV.

range $2.5 < y < 4.0$ are:

$$\begin{aligned}
\sigma_{\text{prompt}} &= 4.79 \ \pm 0.22_{\text{exp}} \ \pm 0.15_{\text{inter}} \ = 4.79 \ \pm 0.27\,\mu\text{b}, \\
\sigma_b &= 0.468 \pm 0.036_{\text{exp}} \pm 0.012_{\text{inter}} = 0.468 \pm 0.038\,\mu\text{b}, \\
\sigma_{\text{incl}} &= 5.27 \ \pm 0.24_{\text{exp}} \ \pm 0.15_{\text{inter}} \ = 5.27 \ \pm 0.28\,\mu\text{b}.
\end{aligned}$$

Ignoring correlations reduces the experimental uncertainty by about 11% for prompt and inclusive J/ψ production and by about 7% for J/ψ from b hadron decays; the total uncertainties would generally be about 7% smaller.

Table 4: Interpolated values of $\sigma(J/\psi)$ (μb) at $\sqrt{s} = 5.02$ TeV for LHCb. The quoted uncertainties are experimental.

	interpolated cross-sections (μb)		
model	prompt J/ψ	inclusive J/ψ	J/ψ from b
linear	4.68 ± 0.21	5.15 ± 0.23	0.473 ± 0.031
power law	4.79 ± 0.22	5.27 ± 0.24	0.468 ± 0.036
exponential	4.94 ± 0.25	5.42 ± 0.27	0.481 ± 0.031

3 Differential cross-section interpolation in ALICE

A study of the y-dependence of $R_{p\mathrm{Pb}}$ was performed by ALICE. Such a study requires the evaluation of $\mathrm{d}\sigma/\mathrm{d}y$ for inclusive J/ψ at $\sqrt{s} = 5.02$ TeV. Data on $\mathrm{d}\sigma/\mathrm{d}y$ in pp collisions are available at $\sqrt{s} = 2.76$ [9] and 7 TeV [10], in the $2.5 < y < 4.0$ region, in six rapidity bins. The rapidity coverage for pPb collisions is $2.03 < y < 3.53$ and $-4.46 < y < -2.96$, and each of the two ranges was also studied in six bins of rapidity. Due to the rapidity shift induced by the asymmetry in the energy of the beams, the pPb ranges do not overlap completely with those explored in pp collisions.

A two-step procedure was followed. First, the interpolation procedure described before was applied to each of the rapidity bins studied in pp collisions, to obtain $\mathrm{d}\sigma/\mathrm{d}y$ at $\sqrt{s} = 5.02$ TeV for $2.5 < y < 4.0$ in six bins. The values are summarized in Tab. 5 and shown in Fig. 5 (left).

The values for $\mathrm{d}\sigma/\mathrm{d}y$ corresponding to the rapidity bins studied in pPb collisions were then obtained by a further interpolation/extrapolation procedure. In more detail, the distribution of the values shown in the left hand plot of Fig. 5 was fitted using several empirical functions, including a Gaussian shape, a second- and a fourth-order polynomial [20]. In the fit procedure, the statistical and y-uncorrelated systematic uncertainties were taken into account. A 5.4% y-correlated uncertainty was then added in quadrature to the uncertainties obtained from each of the fits. This value comes from the quadratic sum of two sources: (i) a 5% uncertainty, originating from the same size $\sqrt{s}$-correlated uncertainty introduced in the first step of the interpolation procedure (we assume here that the uncertainty correlation vs $\sqrt{s}$ shifts the points in the same direction for all the y-bins under study); (ii) a 2% uncertainty, related to the average spread of the values obtained when using the various phenomenological functions (linear, power law and exponential) in the first step of the interpolation. The results are shown in the right hand plot of Fig. 5.

The $\mathrm{d}\sigma/\mathrm{d}y$ values for the binning studied in pPb collisions were then obtained by integrating the fit functions in the corresponding y-ranges. The values, quoted in Tab. 6, correspond to the average of the results obtained with the three fits.

CEM calculations were also performed differentially in rapidity for the bins under study, and their results were used to determine a further, theory-related uncertainty, following the procedure detailed in Section 2.2. The uncertainty values are also reported in Tab. 6. It is worth noting that the uncertainties are significantly larger in the rapidity regions where

Table 5: Interpolation of $\mathrm{d}\sigma/\mathrm{d}y$, using ALICE data. The quoted uncertainties for the experimental data are statistical and systematic, respectively. For the interpolated values, the first uncertainty is related to the total uncertainties of the 2.76 and 7 TeV data, while the second is extracted from the dispersion of the results corresponding to the various fitting functions.

	$\mathrm{d}\sigma/\mathrm{d}y$ (μb)		
	$\sqrt{s} = 2.76$ TeV	$\sqrt{s} = 5.02$ TeV (interpolated)	$\sqrt{s} = 7$ TeV
$2.50 < y < 2.75$	3.05±0.35±0.25	4.65±0.43±0.12	5.85±0.13±0.61
$2.75 < y < 3.00$	2.37±0.19±0.19	4.01±0.36±0.04	5.37±0.06±0.59
$3.00 < y < 3.25$	2.26±0.15±0.18	3.64±0.33±0.06	4.73±0.05±0.55
$3.25 < y < 3.50$	2.01±0.14±0.16	3.29±0.30±0.05	4.32±0.05±0.51
$3.50 < y < 3.75$	2.00±0.16±0.16	3.08±0.28±0.07	3.90±0.05±0.44
$3.75 < y < 4.00$	1.68±0.19±0.13	2.68±0.24±0.05	3.47±0.08±0.35

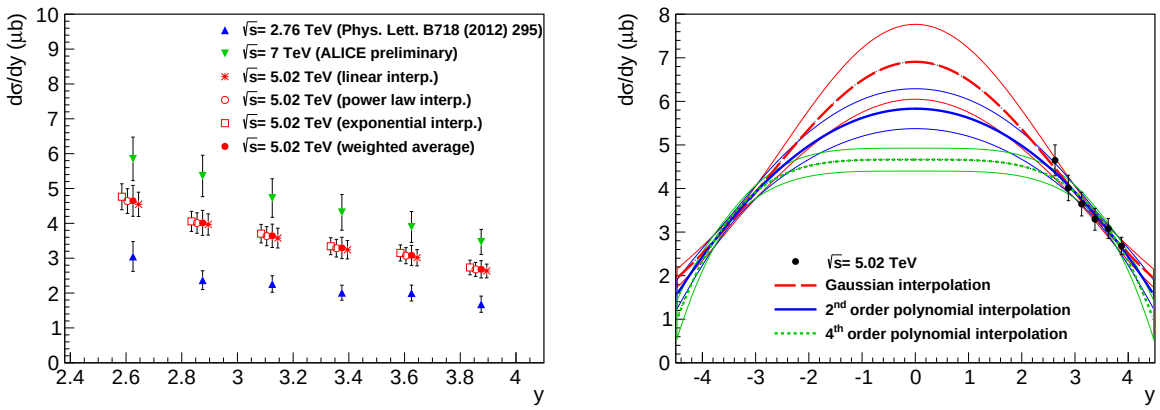

Figure 5: Differential cross-sections $\mathrm{d}\sigma/\mathrm{d}y$ at $\sqrt{s} = 2.76$ and 7 TeV, as measured by ALICE. On the left hand plot the calculated values at $\sqrt{s} = 5.02$ TeV are separately shown for each interpolation function (linear, power law and exponential), together with their weighted average. The right hand figure shows fits to the interpolated $\mathrm{d}\sigma/\mathrm{d}y$ values at $\sqrt{s} = 5.02$ TeV. See text for details.

an extrapolation with respect to the measured pp data is performed. This is particularly evident for the $2.03 < y < 2.28$ and $-4.46 < y < -4.21$ intervals which lie completely outside the pp y-range.

The $\mathrm{d}\sigma/\mathrm{d}y$ values corresponding to the integrated ranges $2.03 < y < 3.53$, $-4.46 < y < -2.96$ have been obtained following the same procedure, and are also reported in Tab. 6.

Table 6: Interpolated $\mathrm{d}\sigma/\mathrm{d}y$ at $\sqrt{s} = 5.02\,\mathrm{TeV}$, for the rapidity intervals corresponding to the binning adopted by ALICE in pPb studies. The first quoted uncertainty is related to the uncorrelated uncertainty obtained in the first step of the interpolation procedure. The second one is the y-correlated uncertainty, while the third one comes from the maximum spread between the results obtained with the three interpolating functions. The last uncertainty represent the theory-related contribution.

	$\mathrm{d}\sigma/\mathrm{d}y$ (μb), $\sqrt{s} = 5.02\,\mathrm{TeV}$
$2.03 < y < 2.28$	4.72±0.28±0.26±0.42±0.12
$2.28 < y < 2.53$	4.53±0.25±0.25±0.24±0.11
$2.53 < y < 2.78$	4.30±0.20±0.23±0.11±0.04
$2.78 < y < 3.03$	4.02±0.16±0.22±0.01±0.11
$3.03 < y < 3.28$	3.70±0.12±0.20±0.04±0.09
$3.28 < y < 3.53$	3.36±0.10±0.18±0.06±0.08
$2.03 < y < 3.53$	4.12±0.18±0.23±0.11±0.10
$-3.21 < y < -2.96$	3.81±0.13±0.21±0.03±0.09
$-3.46 < y < -3.21$	3.47±0.11±0.19±0.06±0.09
$-3.71 < y < -3.46$	3.11±0.11±0.17±0.04±0.03
$-3.96 < y < -3.71$	2.70±0.15±0.15±0.02±0.03
$-4.21 < y < -3.96$	2.30±0.21±0.13±0.10±0.06
$-4.46 < y < -4.21$	1.95±0.26±0.11±0.15±0.05
$-4.46 < y < -2.96$	2.86±0.13±0.16±0.05±0.07

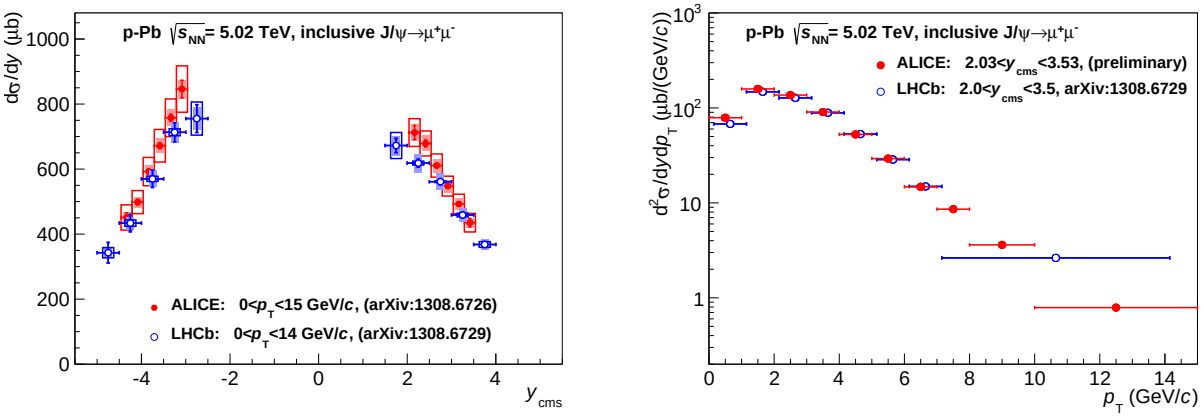

Figure 6: Differential cross-section for inclusive J/ψ production in pPb collisions as a function of rapidity y (left) and transverse momentum p_{T} (right).

4 Comparison of results by ALICE and LHCb

A comparison of the results is performed for inclusive J/ψ production, where the cross-sections were measured by both experiments. The kinematic ranges used in the comparison

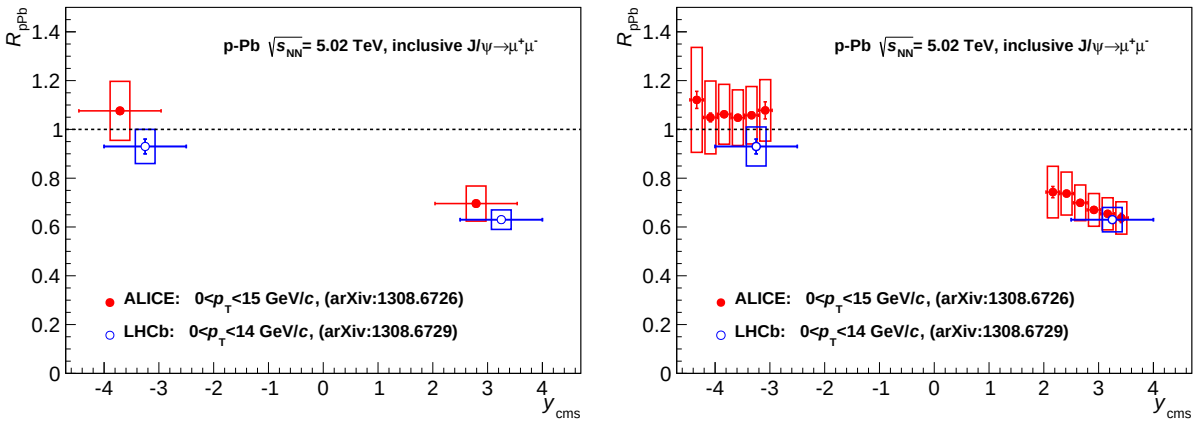

Figure 7: Nuclear modification factor as a function of rapidity. The left hand plot shows the measurements integrated over the accessible kinematic range of both experiments, the right hand plot displays the differential measurement by the ALICE collaboration.

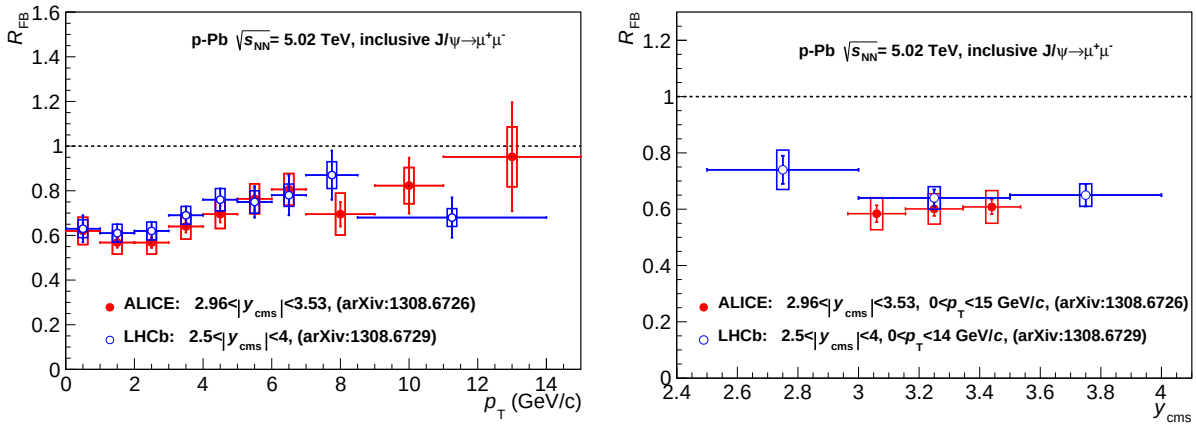

Figure 8: Forward-backward production ratio for inclusive J/ψ production in pPb collisions as a function of p_{T} (left) and as a function of rapidity (right), for both experiments.

are indicated on the plots. Although not identical, they are sufficiently close that a direct comparison is possible.

Figure 6 compares the differential cross-sections for inclusive J/ψ production in pPb collisions measured by ALICE and LHCb, integrated over p_{T} and y, respectively. The differential cross-sections in p_{T} are given only for the forward hemisphere. Within uncertainties, good agreement between both experiments is observed.

The nuclear modification factor as a function of rapidity is shown in Fig. 7. Results integrated over the kinematically accessible rapidity range and a differential measurement by ALICE are shown. The results are compatible, as expected from the agreement of both pPb and interpolated pp cross-sections. The deviation from unity, especially in the forward region, is clear evidence for cold nuclear matter effects affecting J/ψ production

in proton-ion collisions. These are also visible in the forward-backward production ratio as a function of transverse momentum and as a function of rapidity displayed in Fig. 8. A detailed comparison with theoretical predictions is given in the published papers by the ALICE [7] and LHCb [8] collaborations.

5 Summary and conclusions

Measurements of inclusive J/ψ production in pPb collisions performed by the ALICE and LHCb collaborations are in good agreement. The nuclear modification factors and the observed forward-backward production ratios clearly show cold nuclear matter effects. The cross-section interpolations to $\sqrt{s} = 5.02\,\text{TeV}$ in the rapidity range $2.5 < y < 4.0$ have total uncertainty between 5.3 % and 7.9 %.

References

[1] J. Albacete *et al.*, *Predictions for p+Pb collisions at* $\sqrt{s_{NN}} = 5$ TeV, Int. J. Mod. Phys. **E22** (2013) 1330007, arXiv:1301.3395.

[2] N. Brambilla *et al.*, *Heavy quarkonium: progress, puzzles, and opportunities*, Eur. Phys. J. **C71** (2011) 1534, arXiv:1010.5827.

[3] K. Eskola, H. Paukkunen, and C. Salgado, *EPS09: A New Generation of NLO and LO Nuclear Parton Distribution Functions*, JHEP **04** (2009) 065, arXiv:0902.4154.

[4] Z. Conesa del Valle *et al.*, *Quarkonium production in high energy proton-proton and proton-nucleus collisions*, Nucl. Phys. Proc. Suppl. **214** (2011) 3, arXiv:1105.4545.

[5] F. Arleo and S. Peigne, *Heavy-quarkonium suppression in p-A collisions from parton energy loss in cold QCD matter*, JHEP **03** (2013) 122, arXiv:1212.0434.

[6] E. G. Ferreiro, F. Fleuret, J. P. Lansberg, and A. Rakotozafindrabe, *Open-b production in pPb collisions at* $\sqrt{s_{NN}} = 5.02$ TeV: effect of the gluon nuclear densities, as a private communication.

[7] ALICE collaboration, B. Abelev *et al.*, *J/ψ production and nuclear effects in p-Pb collisions at* $\sqrt{s_{NN}} = 5.02$ TeV, arXiv:1308.6726, submitted to JHEP.

[8] LHCb collaboration, R. Aaij *et al.*, *Study of J/ψ production and cold nuclear matter effects in pPb collisions at* $\sqrt{s_{NN}} = 5\,\text{TeV}$, arXiv:1308.6729, submitted to JHEP.

[9] ALICE collaboration, B. Abelev *et al.*, *Inclusive J/ψ production in pp collisions at* $\sqrt{s} = 2.76\,\text{TeV}$, Phys. Lett. **B718** (2012) 295, arXiv:1203.3641.

[10] ALICE collaboration, B. Abelev *et al.*, *Measurement of quarkonium production at forward rapidity in pp collisions at* $\sqrt{s} = 7\,\text{TeV}$ *with the ALICE detector*, in preparation.

[11] LHCb collaboration, R. Aaij *et al.*, *Measurement of* J/ψ *production in pp collisions at* $\sqrt{s} = 2.76\,\text{TeV}$, JHEP **02** (2013) 41, arXiv:1212.1045.

[12] LHCb collaboration, R. Aaij *et al.*, *Measurement of* J/ψ *polarization in pp collisions at* $\sqrt{s} = 7\,\text{TeV}$, Eur. Phys. J. **C73** (2013) 2631, arXiv:1307.6379.

[13] LHCb collaboration, R. Aaij *et al.*, *Production of* J/ψ *and* Υ *mesons in pp collisions at* $\sqrt{s} = 8\,\text{TeV}$, JHEP **06** (2013) 64, arXiv:1304.6977.

[14] J. Wenniger, *Energy Calibration of the LHC Beams at 4 TeV*, CERN-ATS-2013-040 (2013).

[15] Particle Data Group, J. Beringer *et al.*, *Review of Particle Physics*, Phys. Rev. **D86** (2012) 010001, page 447.

[16] M. Zavertyaev, *Empirical parameterization of the high energy behaviour of average charged particle multiplicities in* e^+e^-*, ep and pp collisions*, arXiv:1206.0875.

[17] Glück, M. and Owens, J.F. and Reya, E., *Gluon contribution to hadronic* J/ψ *production*, Phys. Rev. **D17** (1978) 2324.

[18] M. Cacciari, M. Greco, and P. Nason, *The* p_{T} *spectrum in heavy-flavour hadroproduction*, JHEP **9805** (1998) 007, arXiv:hep-ph/9803400.

[19] R. Vogt, J/ψ *production and suppression*, Phys. Rept. **310** (1999) 197.

[20] F. Bossu *et al.*, *Phenomenological interpolation of the inclusive* J/ψ *cross section to proton-proton collisions at 2.76 TeV and 5.5 TeV*, arXiv:1103.2394.